

PALMS: Parallel Adaptive Lasso with Multi-directional Signals for Latent Networks Reconstruction

Zhaoyu Xing *

Paula and Gregory Chow Institute for Studies in Economics,
Xiamen University

Wei Zhong

Department of Statistics & Data Science,
Xiamen University

November 19, 2024

Abstract

Large-scale networks exist in many fields and play an important role in real-world dynamics. However, the networks are usually latent and expensive to detect, which becomes the main challenge for many applications and empirical analysis. Several statistical methods were proposed to infer the edges, but the complexity of algorithms makes them hard to apply to large-scale networks. In this paper, we proposed a general distributed and parallel computing framework for network reconstruction methods via compressive sensing technical, to make them feasible for inferring the super large networks in practice. Combining with the CALMS, we proposed that those estimators enjoy additional theoretical properties, such as consistency and asymptotic normality, we prove that the approximate estimation utilizing the distributed algorithm can keep the theoretical results.

Keywords: Distributed algorithm, Network inferring, Compressive sensing, Evolutionary game, Parallel computing, Network reconstruction

*The authors gratefully acknowledge

1 Introduction

Networks are commonly existing in our world, which characterize the interactions between different items in many fields, such as the social networks between people and the trading networks between companies. With the deepening of research into various complex dynamic systems, network data and network-based dynamic processes have increasingly become focal points of academic inquiry.

From the perspective of empirical analysis, the network structures commonly influence the changes and evolution of the world profoundly (Dhar et al., 2014), like transportation networks between cities, supply chain networks for international trades, and competition relationships in an evolutionary ultimatum game. Many scholars regard the known network structures as a treatment, focusing on whether existing network connections exert an influence on other variables, which is commonly referred to as network effects identification. Examples include the impact of transportation networks on economic development (Bramoullé et al., 2009) and the influence of social networks on U.S. election outcomes (Herzog, 2021; Kleinnijenhuis and De Nooy, 2013). Many topics about the effects of economic networks have also been proposed, such as the externalities that arise from demand and cost linkages (Amiti and Cameron, 2007), the effect of inequality in network centrality (Ghiglino and Goyal, 2010), and the social interactions in networks (Santos et al., 2006, 2008; Choi et al., 2015). In all of these applications, the network structures are assumed to be known, which is necessary for further anal-

ysis based on networks. Many scholars proposed the methodologies and models including the known network structures as new components and embed them into traditional models and frameworks, such as the spatial autoregressive model and its extensions (Zou et al., 2011; Tho et al., 2023). Besides, some researchers employ statistical models to characterize the generating process of networks and use the observed network structures to estimate model parameters, such the exponential-family random graph models (Hunter et al., 2008) and the stochastic block models (Lei, 2016; Lei and Rinaldo, 2015). However, all of these researches require the use of known network structures for model fitting, statistical inference, and prediction.

In the real world, however, large-scale network structures are often latent and inaccessible. The most common reasons are the un-affordable cost of data collection and other practical difficulties such as commercial data privacy and government policy regulations, especially for many empirical studies in economics and finance. Besides, the lack of applicable measurements of network structures and the ambiguity in the interactions between network nodes create many difficulties for network analysis (Boucher and Fortin, 2016), especially for social and political networks (He and Duan, 2018). Although several experimental designs are proposed to identify the unknown network structures (Ma and Goryanin, 2008; Wang et al., 2021) for biochemical topics, they are too expensive and labor-intensive to handle the detection of large-scale networks. These limitations make the network reconstruction problem an meaningful topic.

Network reconstruction aim to infer the latent network structure based only

on observed nodal dynamics. As the nodal features are commonly treated as the dynamics generated with the fixed but latent networks based on some theoretical models, e.g. the evolutionary games (Wang et al., 2021), the synchronization models (Acebrón et al., 2005) and resistor network model (Wang and Lai, 2009), the network reconstruction is known as a challenging “inverse problem”.

To address the network reconstruction problem, several approaches leveraging compressive sensing have been introduced to infer large-scale networks. These group of methods reformulate the network reconstruction task as an optimization problem combining both the latent networks structure and the observed dynamics, and estimate the set of edges by solving the optimization problem with respect to the adjacency matrix of the latent networks (Wang et al., 2011; Han et al., 2015). Although several modifications are proposed with appropriate theoretical properties (Xing et al., 2024), this framework requires a complex transformation of the dynamic data and conduct the optimization algorithms based on a huge transferred dataset. That is, the complexity and the requirements of memory of these algorithms are sensitive to the size of the networks, which makes it almost infeasible for large-scale networks, such as email networks, protein-protein networks and online social networks. Although some distributed algorithm are proposed in the field of computer science, such as distributed ADMM (Lynch, 1996; Tel, 2000; Matamoros et al., 2015; Zhang and Kwok, 2014; Liu et al., 2023), they are proposed for independent observations and utilizing the data-splitting for parallel computing, which is not applicable for network data. Also, the theoretical prop-

erties the estimator based on these distributed optimization algorithms are not clearly justified.

Motivated by these limitations of existing methods for network reconstruction, we propose a new distributed methods to solve the network reconstruction problem namely Parallel Adaptive Lasso with Multi-directional Signals (PALMS). Practically, PALMS can estimate the latent network structures effectively with well-designed sampling process and parallel computing via the multi-directional penalization. Theoretically, we prove the oracle properties of the distributed estimator PALMS while have the adaptive structures in the sub-optimization of the sub-networks. Besides, PALMS can also be treated as a general distributed framework for most of the network reconstruction methods via compressive sensing to reduce the computing time while achieving similar accuracy. And we show that the theoretical properties of the compressive sensing methods, e.g. consistency and asymptotic normality, will be maintained while using PALMS as a distributed framework.

The paper organized as follows: we introduce the background of network reconstruction problem with two classic network dynamic model in Chapter 2. The methodology of PALMS and the theorem are proposed in Chapter 3 and the algorithm of PALMS is proposed in Chapter 4. We show the excellent finite-sample performance of PALMS based on simulations in Chapter 5 and apply our methods to several empirical analysis in Chapter 6. We conclude and list the future topics in Chapter 7. The proofs of the theorem are included in the Appendix.

2 Preliminaries

Evolutionary game theory is a framework used to study the strategic interactions within a population of agents who adjust their behaviors according to evolutionary dynamics, and it is shown to have the power to model complex dynamic system based on networks (Traulsen and Glynatsi, 2023; Wang et al., 2021; Nowak, 2006; Frey, 2010). Evolutionary game theory is widely used in biology, economics, and sociology to model phenomena where agents might not necessarily act rationally (Gatenby and Vincent, 2003; McGill and Brown, 2007; Hummert et al., 2014).

The Ultimatum Game (UG) in networks is one of the famous evolutionary game model used to study the dynamics of players' strategies and deposits within a network structure. In this setting, participants are represented as nodes in a network, and the edges represent the interaction relationships between pairs of participants. In each round of the UG, one participant of a pair acts as the proposer and another as the responder, they need to decide the fraction to share a given amount of deposits without any communication. Specifically, the proposer will propose a fraction $p \in [0, 1]$ for sharing, that is only $1 - p$ of the deposit is shared to the responder. And then responder need to decides whether to accept or reject the offer based on a minimum accept fraction q . If the proposal is rejected, both of them gain 0 from this round of games.

Intuitively, the positions of the proposer and responder are not equal. There-

fore, we consider a fair game process in which, for each round of the game based on each edge of the network, both participants take turns playing the roles of proposer and responder. So for each round of the balanced UG within one pair of participants, there are in total four potential outcomes. Let denote the two participants as i and j , and their strategy pair as (p_i, q_i) and (p_j, q_j) respectively, where each contains one-round proposal p and one-round minimum acceptable fraction q . And then the four potential outcomes could be expressed as:

$$P_{ij} = \begin{cases} p_j + 1 - p_i, & p_i \geq q_j, \quad p_j \geq q_i; \\ 1 - p_i, & p_i \geq q_j, \quad p_j < q_i; \\ p_j, & p_i < q_j, \quad p_j \geq q_i; \\ 0, & p_i < q_j, \quad p_j < q_i. \end{cases} \quad (1)$$

As all the participants are located in a network as nodes, and each edge represents the balanced two-plays, one node (participant) with degree d will play d -round of balanced UG independently with d direct neighbors, and the total income of the node (participant) is the summation of the income in each round of games. Thus, the dynamics on nodal income and strategy-pair in t -th round of game can be concluded in the following formula

$$Y_i^t = \sum_{j=1}^k a_{ij} P_{ij}^t, \quad i = 1, \dots, k, \quad (2)$$

where a_{ij} is the element of adjacency matrix, which represents the network structure of the UG. As the formula 2 shows, the network structure plays an important role in this complex dynamic system.

The Kuramoto model is a mathematical model that describes the synchronization of coupled oscillators. It is originally used to understand how collective behavior arises from the interactions of individual oscillating elements. However, the model is now particularly known for explaining the transition from incoherence to synchronized behavior in systems such as neuronal networks, power grids, and even flocks of birds.

Consider N coupled oscillators, where each oscillator i is characterized by its phase $\theta_i(t)$ and natural frequency ω_i . The dynamics of the Kuramoto model are described by the following set of differential equations:

$$\frac{d\theta_i}{dt} = \omega_i + \sum_{j=1}^N a_{ij} \sin(\theta_j - \theta_i), \quad i = 1, 2, \dots, N, \quad (3)$$

where a_{ij} is from the adjacency matrix representing the coupling relationships between oscillators, and we assume the strength of interaction between the oscillators are identical. The right hand side of equation (3) is the rate of change for each nodes, which is effected by the direct neighbors of the oscillator a_{ij} and the difference in their phase $\sin(\theta_j - \theta_i)$. Thus, the network structure also determine the dynamics of the whole systems, when we treat both the phase and it's rate of change as nodal features.

In both the evolutionary game and synchronization model, the networks are usually given in previous empirical analysis as a part of experimental design. However, in many real-world dynamic systems the network structures are latent but have significant effects. We address the challenging problem to infer the network

structure based only on the observed nodal dynamics. We formally introduce the model settings and our methodology in the Section 3.

3 Model Settings

We consider a fixed networks \mathbf{A} with N nodes, the nodal dynamic $\Psi \in \mathbb{R}^{N \times N}$ and nodal response $Y \in \mathbb{R}^{N \times 1}$, and independent random errors $\epsilon \in \mathbb{R}^{N \times 1}$. Then the network dynamics for t -th round of network dynamics could be expressed as

$$Y^t = (\mathbf{A} \circ \Psi^t) \mathbf{1} + \epsilon^t \quad (4)$$

where \circ is Hadamard product and $\mathbf{1} = [1, \dots, 1]'$. Note that the evolutionary games in networks is a special case of (4) with $\Psi^t = \{P_{ij}^t\}$, and the Kuramoto model in networks is a special case of (4) with $Y^t = [\frac{\Delta \theta_i^t}{h}]$ and $\Psi^t = \{\sin(\theta_i^t - \theta_j^t)\}$, h is sampling interval. Both the evolutionary games and the Kuramoto model are representative example for network dynamics (Wang et al., 2011; Han et al., 2015; Shi et al., 2021; Xing et al., 2024).

Now we consider the distributed algorithm with the estimations based on different sub-networks by randomly grouping the nodes and corresponding edges. Let's denote the indexes of grouped nodes as Δ , then the dynamics related to selected nodes is Y^Δ , the adjacency of sub-network is \mathbf{A}^Δ , and the potential influential values is Ψ^Δ . Then we consider the network reconstruction estimators

based on nodal network dynamics with the following general objective function

$$\tilde{\mathbf{A}}^\Delta = \arg \min_{\mathbf{A} \in \mathbb{R}^{N \times N}} l(\mathbf{Y}^\Delta, \boldsymbol{\Psi}^\Delta), \quad (5)$$

where $l(\cdot)$ is a general loss function which could include well-designed penalties. Many existing network reconstruction methods could be treated as the special cases (??). Some of the estimators $\tilde{\mathbf{A}}$ enjoy the theoretical properties, such as the consistency and asymptotic normality of ALMS and CALMS.

For distributed algorithm, we aim to decompose the network reconstruction problem into several simpler tasks and jointly consider the estimations based on all the outputs from different computing units. Let's consider the m rounds of node-splitting into k different groups, and the estimations of adjacency matrix based on different groups of sub-networks as $\{\tilde{\mathbf{A}}_{(1)}^\Delta, \dots, \tilde{\mathbf{A}}_{(m)}^\Delta\}$. Then the distributed estimator of latent networks are defined as

$$\hat{\mathbf{A}} = \frac{1}{m} \sum_{l=1}^m \hat{\mathbf{A}}_{(l)} \quad (6)$$

Based on the powerful adaptive multi-directional penalization, we proposed our distributed PALMS as

$$\hat{\mathbf{A}}_{PALMS} = \frac{1}{m} \sum_{l=1}^m \hat{\mathbf{A}}_{(l)} \quad (7)$$

$$\hat{\mathbf{A}}_{(l)} = \bigcup_{p,q=1}^k \{\tilde{\mathbf{A}}_{(l)}^{\Delta(p,q)}\} \quad (8)$$

$$\tilde{\mathbf{A}}_{(l)}^{\Delta(p,q)} = \arg \min_{\mathbf{A}_s} \|\mathbf{Y}_{(l)}^{\Delta(p,q)} - (\mathbf{A}_s \circ \boldsymbol{\Psi}_{(l)}^{\Delta(p,q)}) \mathbf{1}\|_F + P_\lambda(\mathbf{A}_s) \quad (9)$$

where Δ represents the index for sub-networks and (l) stands for the l -th splitting of data in the first step of Algorithm A1, k is the number of groups, \bigcup is the union of the estimations based on sub-networks, $P_\lambda(\mathbf{A}_s)$ is the adaptive multi direction penalty defined as

$$P_\lambda(\mathbf{A}) = \lambda \sum_{i,j} w_{ij} \min\{|A_{ij}|, |A_{ij} - 1|\} \quad (10)$$

where w_{ij} is the adaptive weights. The details of the weights and discussions could be found in Xing et al. (2024); Zou (2006).

We could show that under mild conditions, the aggregate estimator $\hat{\mathbf{A}}$ could keep the theoretical results asymptotically for $\tilde{\mathbf{A}}$, such as the consistency and asymptotically normality. Thus, based on the estimator in (9), we show the PALMS estimator is consistent and asymptotically normal in Theorem 1 and Theorem 2.

Theorem 1 (Consistency). *Under the assumptions 5 and assumption 6 in appendix and denote the true latent network structures as \mathbf{A}^* , when the overall estimator defined in (5) is consistent, the PALMS estimator defined in (7) satisfies*

$$\hat{\mathbf{A}} \xrightarrow{p} \mathbf{A}^*$$

Theorem 2 (Asymptotically normality). *Under the assumptions 5 and 6 in appendix and denote the true latent network structures as \mathbf{A}^* , we consider an estimator defined in (5) which is asymptotically normal. Let $\text{vec}(\tilde{\mathbf{A}}) \xrightarrow{d} N(\text{vec}(\mathbf{A}^*), \Sigma)$,*

then for the PALMS estimator defined in (7) satisfies

$$\sqrt{n}(\hat{A}_{ij} - A_{ij}^*) \xrightarrow{d} N(0, V(\boldsymbol{\sigma}, \bar{\rho}))$$

where m is the repeats of splitting, where \hat{A}_{ij} is the estimated edge between item i and item j , $V(\boldsymbol{\sigma})$ and $\bar{\rho}$ are given in the appendix.

When the consistency of the, When we take only $m = 1$, then the asymptotic variance of PALMS estimator is the same as the estimator defined in 9. When we have $m \rightarrow \infty$, the asymptotic variance will becomes $\frac{\bar{\rho}}{2}\boldsymbol{\Sigma}_{c,c}$ which is smaller than the one-round estimation.

4 Algorithm

We state the pseudo-code of distributed network reconstruction algorithm in Algorithm A1. Note that besides of the parameters for each network reconstruction algorithms, we have two hyper-parameters for the distributed network reconstruction algorithms: the number of network splitting m and the size of each sub-network $n = \frac{N}{k}$, where k is the number of parallel computing in step 3 of Algorithm A1. The choice of the sub-networks size n is a classic “bias-and-computational cost” trade-off, the estimation with larger n will have higher accuracy and larger computing cost. And the Algorithm A1 becomes the one-round reconstruction using the classic methods, e.g. Signal Lasso or CALMS, when we choose $n = N$ and $k = 1$. It worth nothing that the m needs to be at least 1

such that the union of sub-networks can cover the original networks. Usually the larger m will give a better aggregated estimation, as shown in the asymptotic variance in Theorem 2, however, the marginal benefit of m will decrease dramatically. Another note that the choice of k matters to the computing time for a specific problem, as a larger k meanings more splitting and shorter computing times for each sub-networks. However, the network splitting takes times. And also there are probably some outliers appear when sub-networks are too small and k is too large.

Algorithm A1 Distributed network reconstruction algorithm

- 1: **for** $l = 1, \dots, m$ **do**
 - 2: Random split the nodes set of the network into k groups, denote as $\mathcal{G}_1, \dots, \mathcal{G}_k$ such that $\cup_{i=1}^k \mathcal{G}_i = \mathcal{V}$.
 - 3: **for** Parallel compute for $i = 1, \dots, k$ **do**
 - 4: extract the corresponding network dynamics related to the sub-networks \mathcal{G}_i , denoted the dynamic response as \mathbf{Y}^Δ and the nodal dynamics Ψ^{Delta}
 - 5: estimated the network structures of \mathcal{G}_i via $\tilde{\mathbf{A}}^\Delta(\mathbf{Y}^\Delta, \Psi^\Delta)$ which is the classic estimator in (5), e.g. ALMS and CALMS.
 - 6: Calculate the residuals of $R_i = Y^\Delta - \Delta \hat{X}^\Delta$ and $\|R_i\|_2$
 - 7: **end for**
 - 8: **end for**
 - 9: For any dimension of X , calculated the aggregated estimation via (6)
-

The complexity of previous network reconstruction algorithm, e.g. Signal Lasso and CALMS, are beyond $O(rN^3)$ for a latent network with size N and r rounds of dynamics, which can be very large for large-scale networks and long sequences of the dynamics. Besides, as the popular network reconstruction methods, e.g. Signal Lasso and CALMS, are based on the transformed dataset $\Phi \in \mathbb{R}^{Nr \times N^2}$ and update the estimations based on matrix-wise operations, which result in a huge need of the memory space of computing. Thus, it's almost impossible to solve the classic network reconstruction problem on only one computer for large-scale networks. However, with distributed algorithm proposed, we could decomposed the reconstruction of large-scale networks into several independent easy tasks and perform parallel computing with different computing units, and combine the network reconstruction of a small sub-network with n nodes together to infer the whole networks. If we use CALMS as an example, the complexity of the modified PALMS algorithm will be $O(sr n^3)$ which is much more smaller than old one, where $n \ll N$ and s is the number of distributed computing unit. Also, the memory requirements will also be much more smaller from $O(rN^3)$ to $O(rn^3)$. In applications, the limitation of physical memory of computers is always the intensive issue for individual scholars while dealing with the large-scale networks.

5 Simulations

In this chapter, we test the effectiveness of proposed distributed algorithm with different networks reconstruction methods. We would like to show the significant uplift in computing speed by combining our distributed algorithm to traditional network reconstruction methods. Specifically, the methods compared in this Chapter are network reconstruction with Lasso (Han et al., 2015), Signal Lasso (Shi et al., 2021), ALMS & CALMS (Xing et al., 2024), and their parallel-version with our proposed distributed framework in (6) denoted as P-lasso, P-Signal Lasso, PALMS and P-CALMS, respectively.

5.1 Simulation settings

The true network structures are generated based on classic and representative random network models, the Erdős-Rényi (ER) random network model, the Barabási-Albert (BA) scale-free network.

The ER random network model is one of the most fundamental and representative models for homogeneous networks. In this model, each pair of nodes is connected by an edge with a pre-set probability p . This results in a binomial degree distribution where the degree of each node follows the binomial distribution $P(k) = \binom{n-1}{k} p^k (1-p)^{n-1-k}$. As n becomes large and p is small, the degree distribution tends to follow a Poisson distribution. We can control the density of simulated networks by the pre-set parameter p in the following examples. The BA

network model is designed to reflect the growth and preferential attachment seen in many real-world networks, such as the hyper-link networks and social networks. The BA model is one of the representative network models for heterogeneous networks, where the degree distribution follows a power law (Albert and Barabási, 2002). That is a small number of nodes have significantly more connections than the majority of nodes. The model starts with an initial set of nodes and, at each time step, a new node is added to the network and connects to existing nodes with a probability proportional to their degree. Networks generated by the BA model are characterized by their scale-free property, which is a feature commonly observed in real-world networks.

For the dynamics generated based on given network structures, we have three settings to test and compare different network reconstruction methods: the evolutionary ultimatum game dynamics, the multi-normal dynamics and the synchronization model dynamics. The details of the dynamic generating process are described as follows.

Data generating process 1: The data are generated based on the evolutionary ultimatum game in networks introduced in previous section. In our evolutionary game model, each player's strategy pair (p_i, q_i) is initially assigned randomly from a standard uniform distribution. At the end of each round, players have the opportunity to update their strategies based on their payoffs. Specifically, the probability that player i adopts a new strategy is given by $(1 + \exp(\frac{Y_i^r - Y_j^r}{N}))^{-1}$, where Y_i^r and Y_j^r are the payoffs of players i and j in round r , and K is a constant

controlling the selection intensity. The payoff matrix $P^{(r)}$ for the r -th round is computed based on Equation (1). To express the payoffs of player i , we rewrite them in the form:

$$Y^t = (\mathbf{A} \circ \mathbf{P}^t)\mathbf{1} + \boldsymbol{\epsilon}^t \quad (11)$$

where $Y_i = (Y_i^1, Y_i^2, \dots, Y_i^r)^\top$ is the vector of payoffs for player i over r rounds, $X_i = (a_{i1}, a_{i2}, \dots, a_{ik})^\top$ represents the connectivity of player i to other players (i.e., the adjacency information), $\Phi_i^{(2)}$ is a matrix whose r -th row corresponds to the payoff coefficients from the payoff matrix $P^{(r)}$ in round r , ϵ_i is a normally distributed random error term following $N(0, 1)$.

For an evolutionary game involving N players over r rounds, the entire dynamics process can be formulated in matrix form as:

$$\mathbf{Y} = \Phi \mathbf{X} + \Xi,$$

where: Y is a stacked vector of all players' payoffs, represented as $Y = (Y'_1, Y'_2, \dots, Y'_n)' \in \mathbb{R}^{rn \times 1}$, where Y_1, Y_2, \dots, Y_n are individual payoffs of the players. Similarly, X is a the vectorization of the adjacency matrix, or stacked vector of all players' connectivity vectors, denoted as $X = \text{vec}(\mathbf{A})$. The matrix Φ is a block-diagonal matrix composed of the individual payoff coefficient matrices, expressed as $\Phi^{(2)} = \text{diag}(\mathbf{P}^1, \mathbf{P}^2, \dots, \mathbf{P}^r) \in \mathbb{R}^{rN \times n(N-1)}$. Finally, Ξ is the vector of random error terms. This formulation captures how each player's payoffs are influenced by their connections with other players and the strategies employed over multiple rounds.

Data generating process 2: The loading matrix $\Phi^{(1)}$ follows a multivariate normal distribution $N_p(\mu, \Sigma)$ with $\mu_j \sim Unif(-1, 1)$, $\Sigma_{jj} \sim Unif(1, 3)$ and $\Sigma_{ij} = 0$ for $i \neq j$. We generate the response by $Y_i = \Phi_i^{(1)}X + \epsilon_i$, where $\epsilon_i \sim N(0, 1)$.

Data generating process 3: The data are generated based on a synchronization model introduced in Section 2. We consider the discrete case and fix time step $h = 0.01$, and generate the data with the following update formula for the t -th step:

$$\frac{y_i^t}{h} = c \sum_{j=1}^N a_{ij} \sin(\theta_j^t - \theta_i^t), \quad (12)$$

where c is a constant for coupling strength. For r discrete changes of k vertices, we define $\phi_{ij}^t = c \sin(\theta_j^t - \theta_i^t)$ and let $Y_i = (y_i^1, \dots, y_i^r)$ and $Y = (Y_1', \dots, Y_k')$, $X_i = (a_{i1}, \dots, a_{ik})$ and $X = (X_1', \dots, X_k')$,

$$\Phi_i^{(3)} = \begin{pmatrix} \phi_{i1}^1 & \phi_{i,2}^1 & \cdots & \phi_{ik}^1 \\ \phi_{i1}^2 & \phi_{i,2}^2 & \cdots & \phi_{ik}^2 \\ \vdots & \vdots & \vdots & \vdots \\ \phi_{i1}^r & \phi_{i,2}^r & \cdots & \phi_{ik}^r \end{pmatrix} \quad (13)$$

and $\Phi^{(3)} = \text{diag}(\Phi_1^{(3)}, \dots, \Phi_k^{(3)})$. The final simulated data are generated from $Y = \Phi^{(3)}X + \Xi$.

5.2 Evaluations

To compare the contributions of distributed computation in network reconstruction, we have selected the following evaluation metrics to compare the per-

formance of different methods in the simulations:

- CPU Time (Time): This metric excludes the time for data pre-processing (i.e., data format conversion) and only considers the CPU time used for completing network reconstruction estimations by each algorithm, measured in seconds.
- Mean Square Error (MSE) of Network Reconstruction: This metric is used to measure the magnitude of the overall network reconstruction error, calculated using the following formula

$$MSE(\hat{X}) = \frac{\sum_{j=1}^p (X_j - \hat{X}_j)^2}{p}.$$

- Success Rates for Nonexistent Links (SRNL): This metric is used to measure the accuracy of the overall network reconstruction for empty edges, calculated by the ratio between the number of correctly predicted nonexistent links and the total number of nonexistent links:

$$ED_0(\hat{X}) = \frac{\sum_{j=1}^p I(X_j = 0)I(\hat{X}_j = 0)}{\sum_{j=1}^p I(X_j = 0)}.$$

- Success Rates for Existing Links (SREL): this metric is used to measure the accuracy of the overall network reconstruction for existing edges, calculated by the ratio between the number of correctly predicted links and the total number of links:

$$ED_1(\hat{X}) = \frac{\sum_{j=1}^p I(X_j = 1)I(\hat{X}_j = 1)}{\sum_{j=1}^p I(X_j = 1)}.$$

For each simulation settings, we repeats for 50 times and report the averages and corresponding standard deviations in the following tables. The details of settings and comparisons are shown in the captions.

5.3 Simulation results based on ER network

We firstly compare the performance of different network reconstruction methods on the network dynamics generated based on different models and show the results in Table 4. It worth nothing that the distributed algorithms PALMS have a significantly shorter computing time in all simulated examples compared to the CALMS based on the whole networks. While achieving the high computational efficiency, the PALMS can achieve a similar accuracy of network reconstructions in terms of the MSE in both simulated examples based on evolutionary games and synchronization models.

We check the effectiveness of distributed framework with increasing number of nodes in networks and show the result in Table 2. As the size of network increases, the computing time of the traditional network reconstruction algorithm, like Signal lasso, ALMS and CALMS, increase largely with only one computing unit. As we analyzed in Chapter 3, the complexity of those algorithms are usually larger than $O(N^3)$. When we apply the distributed network reconstruction algorithm, the computing speed increases largely for any given size of the networks. And the CPU times for distributed algorithms are relatively not so sensitive to growing

networks.

In Table 3, we check the performance and computing cost for reconstruction algorithms for networks with different expected density. When the number of connected edges is large, the observed nodal dynamics would become more complex compared to the dynamics generated from a sparse network. Thus, the individual algorithm needs more updates for convergence. Many network reconstruction methods based on ADMM optimization may not converge very quick, which leads to an increase CPU Times for inferring the complex network structures. Consistently with the previous example in Table 2, the distributed network reconstruction algorithm gives a uplift of computing speed largely in every settings. Besides, the Lasso (Han et al., 2015) have almost no power to give the 1 estimates and the methods based on multi-penalties (Signal lasso, ALMS and CALMS) achieve more accurate estimations for all the cases, which is coincide with the results in previous work (Xing et al., 2024).

We also investigate the good choice of two parameter k and m . As we introduced in Chapter 1, the choice of k is a trade-off between bias and computational complexity. If we choose a large k , the the size of sub-network will be small and the computing time will be shorter by parallel algorithm. And if we choose $k = 1$, then the distributed algorithm reduce to the CALMS as there's no sub-sampling process. When $m > 1$, there will be some correlation between the estimators for one edge, as their sub-networks may possible included the same dynamics. Although, the asymptotic variance of the aggregated variance will decrease with increasing

DGP	method	MSE	sd	CPU Time	sd	SRNL	sd	SREL	sd
eg	Lasso	0.731	0.008	160.783	120.829	1.000	0.001	0.000	0.000
	P-lasso	4.950	2.207	0.340	0.083	0.960	0.006	0.000	0.000
	Signal Lasso	0.283	0.011	38.802	2.019	0.107	0.017	0.580	0.030
	P-Signal Lasso	0.308	0.011	11.546	2.443	0.122	0.021	0.902	0.009
	ALMS	0.386	0.015	512.779	78.636	0.385	0.020	0.698	0.020
	CALMS	0.386	0.015	512.779	78.636	0.385	0.020	0.698	0.020
	PALMS	0.330	0.014	43.386	16.490	0.178	0.015	0.851	0.021
	P-CALMS	0.338	0.016	43.386	16.490	0.200	0.011	0.831	0.023
mvn	Lasso	0.500	0.013	0.081	0.012	1.000	0.001	0.000	0.000
	P-lasso	1.316	0.340	0.546	0.052	0.967	0.006	0.000	0.000
	Signal Lasso	0.310	0.006	37.671	1.700	0.078	0.026	0.087	0.018
	P-Signal Lasso	0.476	0.006	14.563	0.710	0.810	0.041	0.237	0.047
	ALMS	0.472	0.010	1100.440	54.803	0.530	0.012	0.526	0.010
	CALMS	0.472	0.010	1100.440	54.803	0.530	0.012	0.526	0.010
	PALMS	0.460	0.009	34.173	3.239	0.538	0.015	0.543	0.005
	P-CALMS	0.460	0.010	34.173	3.239	0.545	0.018	0.535	0.007
syn	Lasso	0.242	0.023	0.125	0.027	0.998	0.004	0.000	0.000
	P-lasso	0.479	0.052	0.544	0.103	0.981	0.006	0.000	0.000
	Signal Lasso	0.229	0.012	36.427	0.187	0.790	0.090	0.042	0.011
	P-Signal Lasso	0.332	0.018	13.263	0.944	0.802	0.047	0.246	0.063
	ALMS	0.444	0.012	1154.760	41.675	0.559	0.010	0.546	0.034
	CALMS	0.444	0.012	1154.760	41.675	0.559	0.010	0.546	0.034
	PALMS	0.464	0.019	26.902	3.462	0.519	0.022	0.590	0.028
	P-CALMS	0.461	0.018	26.902	3.462	0.524	0.022	0.586	0.026

Table 1: Performance of distributed and non-distributed network reconstruction methods for ER networks and different data-generating processes of network dynamics

N	method	MSE	sd	CPU Time	sd	SRNL	sd	SREL	sd
30	Lasso	1.214	1.241	6.112	10.354	0.997	0.009	0.000	0.000
	P-lasso	0.720	0.024	0.706	0.390	0.964	0.020	0.040	0.012
	Signal Lasso	0.268	0.018	20.052	8.362	0.138	0.036	0.663	0.083
	P-Signal Lasso	0.302	0.028	9.495	3.968	0.149	0.042	0.891	0.040
	ALMS	0.376	0.014	114.274	62.561	0.376	0.033	0.711	0.017
	CALMS	0.376	0.014	114.274	62.561	0.376	0.033	0.711	0.017
	PALMS	0.317	0.015	23.753	11.185	0.187	0.030	0.857	0.016
	P-CALMS	0.328	0.017	23.753	11.185	0.203	0.031	0.836	0.014
40	Lasso	0.752	0.044	19.906	142.343	0.999	0.002	0.000	0.000
	P-lasso	0.713	0.016	0.778	0.395	0.976	0.013	0.027	0.005
	Signal Lasso	0.286	0.014	48.197	21.491	0.108	0.015	0.593	0.043
	P-Signal Lasso	0.304	0.017	18.009	7.041	0.121	0.021	0.912	0.019
	ALMS	0.391	0.018	600.076	325.875	0.380	0.029	0.695	0.024
	CALMS	0.391	0.018	600.076	325.875	0.380	0.029	0.695	0.024
	PALMS	0.324	0.014	45.683	21.068	0.178	0.021	0.863	0.015
	P-CALMS	0.332	0.012	45.683	21.068	0.189	0.022	0.848	0.015
50	Lasso	0.886	0.313	120.437	8952.318	0.996	0.004	0.000	0.000
	P-lasso	0.722	0.007	0.950	0.515	0.981	0.005	0.026	0.005
	Signal Lasso	0.298	0.009	152.129	8.081	0.096	0.014	0.572	0.027
	P-Signal Lasso	0.300	0.011	33.254	14.683	0.119	0.018	0.908	0.018
	ALMS	0.391	0.011	2907.002	1546.948	0.358	0.023	0.699	0.012
	CALMS	0.391	0.011	2907.002	1546.948	0.358	0.023	0.699	0.012
	PALMS	0.332	0.011	104.204	50.769	0.177	0.028	0.844	0.020
	P-CALMS	0.340	0.012	104.204	50.769	0.188	0.029	0.829	0.024

Table 2: Performance of distributed and non-distributed network reconstruction methods for ER networks and evolutionary games' dynamic with changing network size

m , large m will uplift the computing cost directly.

5.4 Simulation results based on BA network

We also test and compare the performance of the different network reconstruction methods based on BA network model. The primary results are similar to the simulations based on EA networks.

Firstly, we compare the performance of network reconstruction with different data-generating process of the network dynamics in Table 5. Similarly to the results in Table 4, Lasso method has no power to estimate the edges exactly, and PALMS could be computed effectively for large-scale networks and the computing times for all cases are much more shorter than CALMS, which is proposed recently with appropriate statistical properties. PALMS gives a more accurate estimation of the network structures, especially for the existing edges, compared to the classic network reconstruction methods.

In Table 6, we generate the samples of the latent true network structure with different network density by controlling the average degree of nodes. We generate the network with 50 nodes and control the average degree around 5 for density setting 0.1, and 20 for density 0.4 and 35 for density 0.7. Based on the simulation results, the PALMS can be computed much faster than the CALMS based on the whole networks, which shows the effectiveness of distributed algorithms. In terms of the MSE, SRNL and SREL, PALMS achieves similar accuracy of network

dense	method	MSE	sd	CPU Time	sd	SRNL	sd	SREL	sd
0.1000	Lasso	0.010	0.003	0.351	0.104	0.984	0.010	0.000	0.000
	P-lasso	0.019	0.006	1.939	0.406	0.984	0.007	0.000	0.000
	Signal Lasso	0.003	0.003	152.668	5.865	0.948	0.015	0.018	0.032
	P-Signal Lasso	0.063	0.025	42.457	3.935	0.945	0.024	0.198	0.125
	ALMS	0.462	0.012	2451.123	204.348	0.539	0.012	0.491	0.110
	CALMS	0.462	0.012	2451.123	204.348	0.539	0.012	0.491	0.110
	PALMS	0.334	0.027	21.243	3.167	0.666	0.027	0.607	0.109
	P-CALMS	0.334	0.027	21.243	3.167	0.666	0.027	0.607	0.109
0.4000	Lasso	0.155	0.013	0.367	0.180	0.997	0.010	0.000	0.000
	P-lasso	0.386	0.164	2.420	0.419	0.977	0.009	0.000	0.000
	Signal Lasso	0.154	0.013	184.385	8.295	0.842	0.081	0.030	0.021
	P-Signal Lasso	0.295	0.039	47.651	5.290	0.781	0.053	0.275	0.050
	ALMS	0.464	0.013	2319.935	136.530	0.538	0.012	0.526	0.033
	CALMS	0.464	0.013	2319.935	136.530	0.538	0.012	0.526	0.033
	PALMS	0.450	0.018	46.679	8.259	0.545	0.020	0.582	0.035
	P-CALMS	0.448	0.017	46.679	8.259	0.548	0.018	0.578	0.038
0.7000	Lasso	0.487	0.035	0.323	0.066	0.997	0.005	0.000	0.000
	P-lasso	1.900	0.529	1.280	0.865	0.960	0.007	0.000	0.000
	Signal Lasso	0.312	0.011	156.863	2.743	0.091	0.023	0.070	0.009
	P-Signal Lasso	0.467	0.010	34.702	14.725	0.706	0.065	0.341	0.078
	ALMS	0.461	0.014	2215.108	137.857	0.535	0.022	0.544	0.011
	CALMS	0.461	0.014	2215.108	137.857	0.535	0.022	0.544	0.011
	PALMS	0.461	0.010	47.880	23.247	0.477	0.022	0.607	0.029
	P-CALMS	0.463	0.011	47.880	23.247	0.483	0.022	0.595	0.028

Table 3: Performance of distributed and non-distributed network reconstruction methods for ER networks and evolutionary games dynamic with different probability p

k	method	MSE	sd	CPU Time	sd	SRNL	sd	SREL	sd
2	Lasso	0.725	0.020	0.360	0.111	1.000	0.000	0.000	0.000
	P-lasso	0.803	0.246	0.463	0.023	0.997	0.009	0.000	0.000
	Signal Lasso	0.284	0.020	104.467	11.227	0.276	0.054	0.742	0.063
	P-Signal Lasso	0.275	0.021	48.774	1.329	0.106	0.046	0.960	0.023
	ALMS	0.341	0.019	572.591	66.444	0.402	0.032	0.755	0.020
	CALMS	0.341	0.019	572.591	66.444	0.402	0.032	0.755	0.020
	PALMS	0.273	0.020	47.047	5.133	0.015	0.010	0.997	0.004
	P-CALMS	0.274	0.020	47.047	5.133	0.015	0.010	0.996	0.004
4	Lasso	0.727	0.018	0.263	0.025	1.000	0.000	0.000	0.000
	P-lasso	56.204	216.269	1.343	0.052	0.955	0.024	0.000	0.000
	Signal Lasso	0.276	0.018	96.364	4.238	0.286	0.032	0.765	0.080
	P-Signal Lasso	0.290	0.012	39.307	0.661	0.133	0.030	0.927	0.020
	ALMS	0.336	0.019	579.226	92.512	0.407	0.037	0.759	0.020
	CALMS	0.336	0.019	579.226	92.512	0.407	0.037	0.759	0.020
	PALMS	0.273	0.018	20.625	2.326	0.003	0.003	1.000	0.002
	P-CALMS	0.280	0.018	20.625	2.326	0.023	0.008	0.982	0.006
6	Lasso	0.720	0.012	0.266	0.021	1.000	0.000	0.000	0.000
	P-lasso	49.634	181.797	2.395	0.694	0.857	0.052	0.000	0.000
	Signal Lasso	0.285	0.012	94.124	3.337	0.290	0.025	0.741	0.051
	P-Signal Lasso	0.301	0.012	37.556	10.572	0.142	0.041	0.915	0.021
	ALMS	0.349	0.018	559.544	78.866	0.399	0.028	0.748	0.019
	CALMS	0.349	0.018	559.544	78.866	0.399	0.028	0.748	0.019
	PALMS	0.279	0.013	16.892	4.630	0.004	0.004	0.999	0.001
	P-CALMS	0.285	0.013	16.892	4.630	0.021	0.012	0.984	0.006

Table 4: Performance of distributed and non-distributed network reconstruction methods for ER networks and different k

DGP	method	MSE	sd	CPU Time	sd	SRNL	sd	SREL	sd
eg	Lasso	0.733	0.000	10.747	13.026	1.000	0.000	0.000	0.000
	P-lasso	1.006	3.411	1.366	0.422	0.988	0.014	0.000	0.000
	Signal Lasso	0.276	0.015	43.453	2.045	0.240	0.043	0.839	0.027
	P-Signal Lasso	0.298	0.021	23.736	6.882	0.094	0.050	0.923	0.037
	ALMS	0.314	0.013	214.465	28.098	0.450	0.025	0.772	0.018
	CALMS	0.314	0.013	214.465	28.098	0.450	0.025	0.772	0.018
	PALMS	0.270	0.006	13.886	4.032	0.018	0.011	0.989	0.009
	P-CALMS	0.271	0.007	13.886	4.032	0.026	0.012	0.984	0.010
mvn	Lasso	0.745	0.030	0.183	0.016	0.996	0.006	0.000	0.000
	P-lasso	2.217	0.730	1.753	0.047	0.956	0.013	0.000	0.000
	Signal Lasso	0.262	0.019	94.136	3.823	0.062	0.041	0.697	0.285
	P-Signal Lasso	0.626	0.023	42.011	0.773	0.819	0.062	0.212	0.034
	ALMS	0.451	0.018	428.343	42.255	0.536	0.025	0.554	0.022
	CALMS	0.451	0.018	428.343	42.255	0.536	0.025	0.554	0.022
	PALMS	0.468	0.022	38.889	1.803	0.523	0.034	0.535	0.023
	P-CALMS	0.474	0.023	38.889	1.803	0.532	0.034	0.524	0.023
syn	Lasso	0.764	0.046	0.274	0.091	0.991	0.010	0.000	0.000
	P-lasso	3.751	1.115	1.760	0.105	0.946	0.024	0.000	0.000
	Signal Lasso	0.256	0.010	88.440	3.610	0.081	0.035	0.593	0.326
	P-Signal Lasso	0.574	0.034	43.698	1.504	0.730	0.104	0.316	0.073
	ALMS	0.443	0.015	478.322	27.752	0.530	0.023	0.567	0.018
	CALMS	0.443	0.015	478.322	27.752	0.530	0.023	0.567	0.018
	PALMS	0.432	0.017	43.185	2.217	0.458	0.041	0.608	0.023
	P-CALMS	0.440	0.016	43.185	2.217	0.468	0.039	0.594	0.024

Table 5: Performance of distributed and non-distributed network reconstruction methods for BA networks and different data-generating processes of network dynamics

reconstruction with CALMS while reduce the computing time to around 10%. When the dynamics are generated based on a dense networks, for the examples with density 0.4 and 0.7, the convergence of all methods become slower and the CPU time are relatively higher compared to the sparse examples.

6 Empirical analysis

We test our proposed distributed methods with several real-world structures, including the email-connection network among the scholars in European institutions¹, the gene interaction network in biological experiments², the protein-protein interaction network³ and the Facebook friendship-relationship network⁴ and Amazon product co-purchasing networks.

The mail-networks dataset is a network dataset generated from email communications within a large European research institution. It provides anonymized information on email exchanges between the institution’s members and highlights how people are connected through their email communications. This large-scale network have 1005 nodes and 25571 edges and 105461 triangles, which includes both internal and external communication links.

The gene network dataset represents a network of gene regulation in the yeast

¹<https://snap.stanford.edu/data/email-Eu-core.html>

²<https://snap.stanford.edu/data/S-cerevisiae.html>

³<http://vlado.fmf.uni-lj.si/pub/networks/data/bio/Yeast/Yeast.htm>

⁴<https://snap.stanford.edu/data/ego-Facebook.html>

Density	method	MSE	sd	CPU Time	sd	SRNL	sd	SREL	sd
0.1	Lasso	0.187	0.002	0.170	0.048	0.999	0.003	0.000	0.000
	P-lasso	0.391	0.105	1.089	0.140	0.975	0.008	0.000	0.000
	Signal Lasso	0.178	0.012	50.548	8.129	0.765	0.177	0.051	0.027
	P-Signal Lasso	0.303	0.035	22.266	3.142	0.788	0.053	0.300	0.070
	ALMS	0.456	0.018	514.531	70.673	0.540	0.018	0.565	0.034
	CALMS	0.456	0.018	514.531	70.673	0.540	0.018	0.565	0.034
	PALMS	0.437	0.010	29.473	4.991	0.562	0.016	0.570	0.038
	P-CALMS	0.434	0.010	29.473	4.991	0.567	0.015	0.564	0.038
0.4	Lasso	0.640	0.037	0.136	0.044	0.994	0.013	0.000	0.000
	P-lasso	1.725	0.721	1.242	0.349	0.961	0.016	0.000	0.000
	Signal Lasso	0.301	0.023	55.481	8.518	0.069	0.029	0.213	0.179
	P-Signal Lasso	0.567	0.031	27.563	6.177	0.838	0.055	0.192	0.059
	ALMS	0.453	0.023	593.770	66.198	0.536	0.037	0.554	0.028
	CALMS	0.453	0.023	593.770	66.198	0.536	0.037	0.554	0.028
	PALMS	0.465	0.015	50.194	12.890	0.542	0.023	0.531	0.028
	P-CALMS	0.469	0.016	50.194	12.890	0.550	0.022	0.520	0.028
0.7	Lasso	0.902	0.053	0.135	0.034	0.996	0.009	0.000	0.000
	P-lasso	3.192	1.559	1.129	0.400	0.953	0.029	0.000	0.000
	Signal Lasso	0.116	0.014	56.043	10.527	0.097	0.045	0.865	0.094
	P-Signal Lasso	0.736	0.027	25.672	8.503	0.833	0.066	0.192	0.036
	ALMS	0.460	0.012	534.231	66.546	0.536	0.037	0.541	0.014
	CALMS	0.460	0.012	534.231	66.546	0.536	0.037	0.541	0.014
	PALMS	0.476	0.011	50.224	12.748	0.544	0.057	0.522	0.013
	P-CALMS	0.483	0.012	50.224	12.748	0.554	0.049	0.513	0.014

Table 6: Performance of distributed and non-distributed network reconstruction methods for BA networks and evolutionary games dynamic with different network density

Saccharomyces cerevisiae. In this network, each node corresponds to an operon, which is a group of genes transcribed together into a single mRNA molecule. The network includes 690 nodes, 1094 directed edges and 72 triangles. A directed edge from operon i to operon j means that i is regulated by a transcriptional factor encoded by j .

The protein-protein interaction network in budding yeast dataset (Bu et al., 2003), consists of a network that represents interactions between proteins in *Saccharomyces cerevisiae* (budding yeast). The dataset includes 2361 vertices (proteins) and 7182 edges (interactions), with 536 loops.

Facebook friendship-relationship network is a collection of anonymity Facebook data that focuses on users' friends lists (Leskovec and Mcauley, 2012). It contains ego networks, which capture the relationships between a user (ego) and their friends (alters), as well as the relationships between those friends. The large network are obtained by merging the ego networks and includes 4039 nodes and 88234 edges. The network has a high average clustering coefficient of 0.6055, indicating that users' friends tend to be friends with each other.

The Amazon product co-purchasing network dataset⁵ is a comprehensive collection of metadata and review information from the Amazon website, detailing 548552 unique products across categories like books, music CDs, DVDs, and VHS tapes. The data collected in the summer of 2006 includes rich details about each product, such as its title, Amazon sales rank, a list of similar items frequently co-

⁵<https://snap.stanford.edu/data/amazon-meta.html>

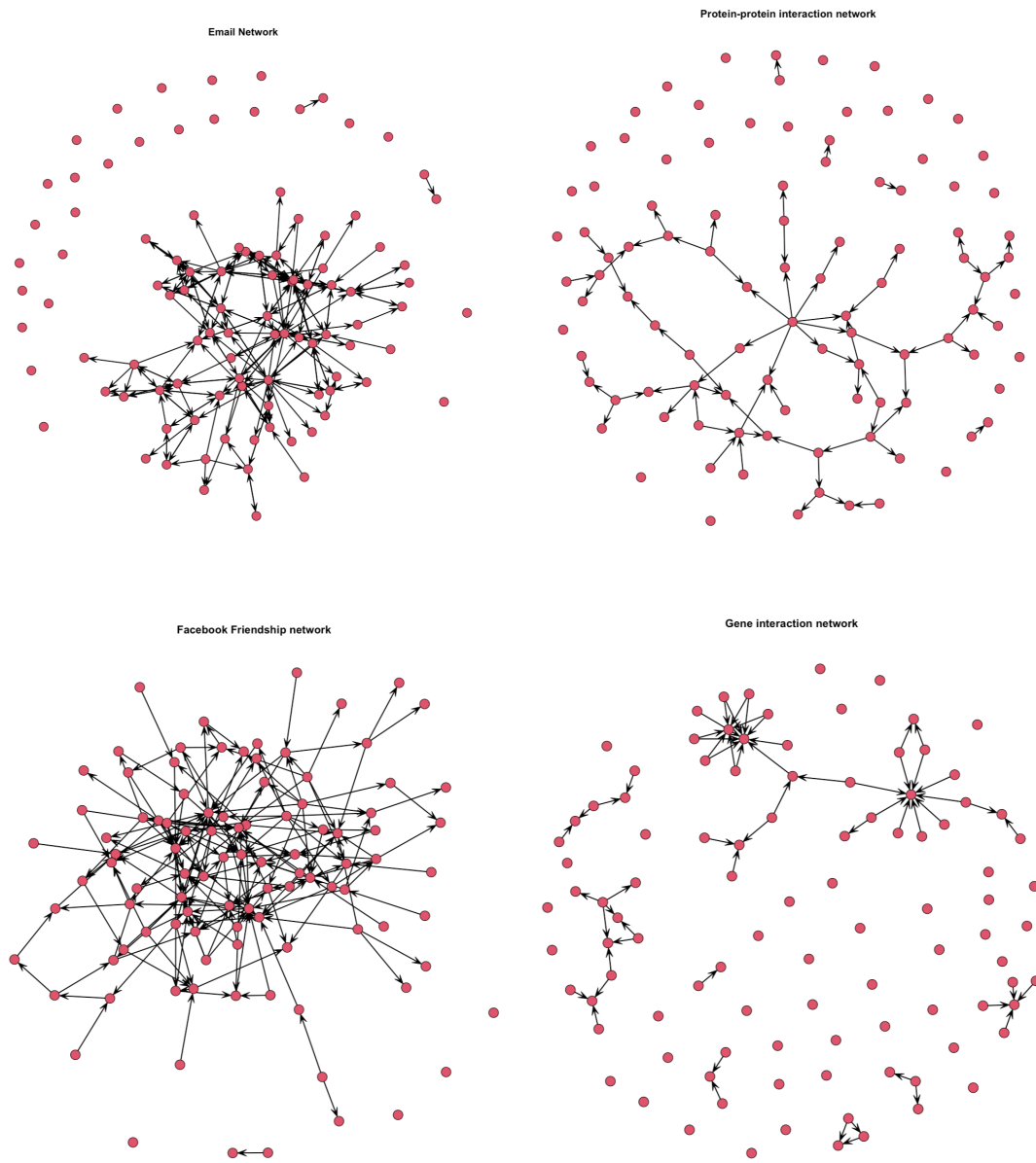


Figure 1: The real-world network structures in empirical analysis

purchased by customers, detailed product categorization, and user reviews. Each node in the network represents one of the product, and the links represent relationships of frequent joint purchases. This dataset has been widely used in studies on product recommendation and marketing dynamics. As the Figure 2 shows that these networks are super large and sparse, we will eliminate the products will no co-purchasing relationships and focus only on the estimation of network structures between DVDs only.

These datasets are collected with large amounts of nodes and complex structures of edges, as the Figure 1 and Figure 2 show, which make the classic network reconstruction methods are not applicable for inferring the latent network structures. Even the first step of the classic method, transforming the dataset, can be challenging due to the limitation of the memory. However, the proposed distributed algorithm could decompose the complex network reconstruction problem into several parallel tasks and utilizing several computing units to estimate the network structures simultaneously. We show the estimation results of PALMS in Table 7.

For the reconstruction problem of the large-scale and sparse network in our empirical analysis, we will compare the performance mainly based on the SREL rather than MSE. Because for the sparse networks with few “1” edges, the MSE can also be extremely small when we just estimate an empty network. However, the identification of the existing edges within the sparse networks is much more challenging. As the results shows, our proposed method PALMS achieves a higher

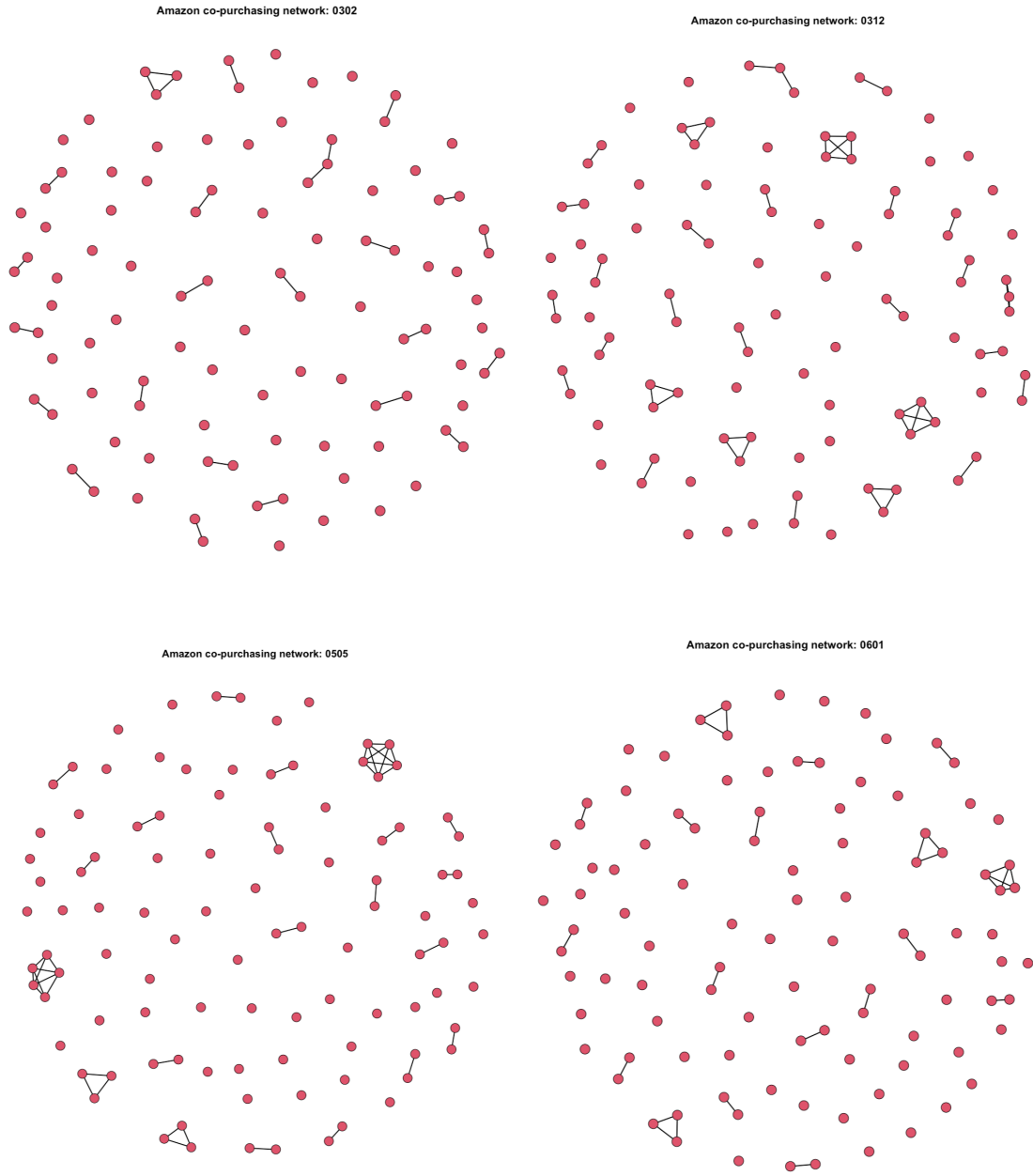


Figure 2: Amazon co-purchasing networks at different times

accuracy in existing edges for all real-world networks structures.

Dataset	Method	SREL	SRNL	MSE
Email network	Lasso	0.0000	1.0000	0.1105
	P-lasso	0.0000	0.9051	7.1571
	P-Signal Lasso	0.5260	0.5831	0.4232
	PALMS	0.9377	0.0638	0.8396
	P-CALMS	0.9221	0.0773	0.8294
Protein-protein interaction network	Lasso	0.0000	1.0000	0.0080
	P-lasso	0.0000	1.0000	0.0080
	P-Signal Lasso	0.5685	0.7222	0.2790
	PALMS	0.7109	0.5747	0.4242
	P-CALMS	0.7109	0.5747	0.4242
facebook network	Lasso	0.0000	1.0000	0.0207
	P-lasso	0.0000	0.9993	0.0225
	P-Signal Lasso	0.7231	0.5808	0.4163
	PALMS	0.8925	0.3535	0.6353
	P-CALMS	0.8925	0.3536	0.6352
Gene network	Lasso	0.0000	1.0000	0.0078
	P-lasso	0.0000	1.0000	0.0078
	P-Signal Lasso	0.7488	0.8398	0.1609
	PALMS	0.8293	0.7752	0.2243
	P-CALMS	0.8293	0.7752	0.2243
Amazon co-purchasing networks	Lasso	0.0000	1.0000	0.0171
	P-lasso	0.0000	1.0000	0.0171
	2nd Mar. P-Signal Lasso	0.5109	0.7160	0.2903
	PALMS	0.5761	0.5620	0.4424
	P-CALMS	0.5761	0.5620	0.4424
	Lasso	0.0000	1.0000	0.0304
	P-lasso	0.0000	1.0000	0.0304
	12th Mar. P-Signal Lasso	0.7848	0.5437	0.4634
	PALMS	0.8797	0.3873	0.6168
	P-CALMS	0.8797	0.3873	0.6168
	Lasso	0.0000	1.0000	0.0290
	P-lasso	0.0000	1.0000	0.0290
	12th Mar. P-Signal Lasso	0.6859	0.5430	0.4640
	PALMS	0.8013	0.4001	0.6041
	P-CALMS	0.8013	0.4001	0.6041
Lasso	0.0000	1.0000	0.0244	
P-lasso	0.0000	1.0000	0.0244	
1st Jun. P-Signal Lasso	0.6988	0.6036	0.4037	
PALMS	0.8373	0.4454	0.5593	
P-CALMS	0.8373	0.4454	0.5593	

35
Table 7: Empirical analysis results

References

- Albert, R., & Barabási, A. L. (2002). Statistical mechanics of complex networks. *Reviews of modern physics*, 74(1), 47.
- Acebrón, J. A., Bonilla, L. L., Pérez Vicente, C. J., Ritort, F., & Spigler, R. (2005). The Kuramoto model: A simple paradigm for synchronization phenomena. *Reviews of modern physics*, 77(1), 137-185.
- Bramoullé, Y., Djebbari, H., & Fortin, B. (2009). Identification of peer effects through social networks. *Journal of econometrics*, 150(1), 41-55.
- He, R., & Duan, X. (2018, April). Twitter summarization based on social network and sparse reconstruction. In *Proceedings of the AAAI Conference on Artificial Intelligence* (Vol. 32, No. 1).
- Hunter, D. R., Handcock, M. S., Butts, C. T., Goodreau, S. M., & Morris, M. (2008). ergm: A package to fit, simulate and diagnose exponential-family models for networks. *Journal of statistical software*, 24(3), nihpa54860.
- Lei, J., & Rinaldo, A. (2015). Consistency of spectral clustering in stochastic block models. *The Annals of Statistics*, 215-237.
- Lei, J. (2016). A goodness-of-fit test for stochastic block models. *The Annals of Statistics*, 44(1), 401.

- Zhang, R., & Kwok, J. (2014, June). Asynchronous distributed ADMM for consensus optimization. In International conference on machine learning (pp. 1701-1709). PMLR.
- Matamoros, J., Fosson, S. M., Magli, E., & Antón-Haro, C. (2015). Distributed ADMM for in-network reconstruction of sparse signals with innovations. *IEEE Transactions on Signal and Information Processing over Networks*, 1(4), 225-234.
- Liu, Y., Huang, K., Yang, C., & Wang, Z. (2023). Distributed network reconstruction based on binary compressed sensing via ADMM. *IEEE Transactions on Network Science and Engineering*, 10(4), 2141-2153.
- Amiti, M., & Cameron, L. (2007). *Economic geography and wages*. *The Review of Economics and Statistics*, 89(1), 15-29.
- Boucher, V., & Fortin, B. (2016). *Some challenges in the empirics of the effects of networks*. *Handbook on the Economics of Networks*, 45, 48.
- Bu, D., Zhao, Y., Cai, L., Xue, H., Zhu, X., Lu, H., ... & Chen, R. (2003). Topological structure analysis of the protein-protein interaction network in budding yeast. *Nucleic acids research*, 31(9), 2443-2450.
- Kleinnijenhuis, J., & De Nooy, W. (2013). Adjustment of issue positions based on network strategies in an election campaign: A two-mode network autoregression model with cross-nested random effects. *Social Networks*, 35(2), 168-177.

- Choi, S., Gallo, E., & Kariv, S. (2015). *Networks in the laboratory*. Cambridge Working Papers in Economics, 1551.
- Dhar, V., Geva, T., Oestreicher-Singer, G., & Sundararajan, A. (2014). *Prediction in economic networks*. *Information Systems Research*, 25(2), 264-284.
- Herzog, I. (2021). National transportation networks, market access, and regional economic growth. *Journal of Urban Economics*, 122, 103316.
- Ghiglini, C., & Goyal, S. (2010). *Keeping up with the neighbors: social interaction in a market economy*. *Journal of the European Economic Association*, 8(1), 90-119.
- Boucher, V., & Fortin, B. (2016). *Some challenges in the empirics of the effects of networks*. *Handbook on the Economics of Networks*, 45, 48.
- Wang, W. X., Ni, X., Lai, Y. C., & Grebogi, C. (2011). *Pattern formation, synchronization, and outbreak of biodiversity in cyclically competing games*. *Physical Review E*, 83(1), 011917.
- Ma, H., & Goryanin, I. (2008). *Human metabolic network reconstruction and its impact on drug discovery and development*. *Drug Discovery Today*, 13(9-10), 402-408.
- Santos, F. C., Santos, M. D., & Pacheco, J. M. (2008). *Social diversity promotes the emergence of cooperation in public goods games*. *Nature*, 454(7201), 213-216.

- Santos, F. C., Pacheco, J. M., & Lenaerts, T. (2006). *Evolutionary dynamics of social dilemmas in structured heterogeneous populations*. Proceedings of the National Academy of
- Wang, H., Robinson, J. L., Kocabas, P., Gustafsson, J., Anton, M., Cholley, P. E., ... & Nielsen, J. (2021). *Genome-scale metabolic network reconstruction of model animals as a platform for translational research*. Proceedings of the National Academy of Sciences, 118(30).
- Wang, W. X., Lai, Y. C., Grebogi, C., & Ye, J. (2011). *Network reconstruction based on evolutionary-game data via compressive sensing*. Physical Review X, 1(2), 021021.
- Zou, T., Luo, R., Lan, W., & Tsai, C. L. (2021). Network influence analysis. *Statistica Sinica*, 31(4), 1727-1748.
- Han, X., Shen, Z., Wang, W. X., & Di, Z. (2015). *Robust reconstruction of complex networks from sparse data*. Physical review letters, 114(2), 028701.
- Nowak, M. A. (2006). *Evolutionary dynamics: exploring the equations of life*. Harvard university press.
- Shi, L., Shen, C., Jin, L., Shi, Q., Wang, Z., & Boccaletti, S. (2021). *Inferring network structures via signal Lasso*. Physical Review Research, 3(4), 043210.
- Matamoros, J., Fosson, S. M., Magli, E., & Antón-Haro, C. (2015). Distributed ADMM for in-network reconstruction of sparse signals with innovations. IEEE

Transactions on Signal and Information Processing over Networks, 1(4), 225-234.

Qu, L., Wang, Z., Huo, Y., Zhou, Y., Xin, J., & Qian, W. (2020, July). Distributed local Bayesian network for gene regulatory network reconstruction. In 2020 6th International Conference on Big Data Computing and Communications (BIGCOM) (pp. 131-139). IEEE.

Leskovec, J., & Mcauley, J. (2012). Learning to discover social circles in ego networks. *Advances in neural information processing systems*, 25.

Wang, W. X., & Lai, Y. C. (2009). Abnormal cascading on complex networks. *Physical Review E—Statistical, Nonlinear, and Soft Matter Physics*, 80(3), 036109.

Wang, X., Wang, M., & Gu, Y. (2015). A distributed tracking algorithm for reconstruction of graph signals. *IEEE Journal of Selected Topics in Signal Processing*, 9(4), 728-740.

Morbidi, F., & Kibangou, A. Y. (2014). A distributed solution to the network reconstruction problem. *Systems & Control Letters*, 70, 85-91.

Zou, H. (2006). The adaptive lasso and its oracle properties. *Journal of the American statistical association*, 101(476), 1418-1429.

Kibangou, A. Y. (2015, August). Distributed network topology reconstruction in

- presence of anonymous nodes. In 2015 23rd European Signal Processing Conference (EUSIPCO) (pp. 215-219). IEEE.
- Pan, W., Sootla, A., & Stan, G. B. (2014). Distributed reconstruction of nonlinear networks: An ADMM approach. *IFAC Proceedings Volumes*, 47(3), 3208-3213.
- Tel, G. (2000). *Introduction to distributed algorithms*. Cambridge university press.
- Lynch, N. A. (1996). *Distributed Algorithms*. Morgan Kaufmann Publishers.
- Breiman, L. (2001). Random forests. *Machine learning*, 45, 5-32.
- Frey, E. (2010). *Evolutionary game theory: Theoretical concepts and applications to microbial communities*. *Physica A: Statistical Mechanics and its Applications*, 389(20), 4265-4298.
- Tho, Z. Y., Ding, D., Hui, F. K., Welsh, A. H., & Zou, T. (2023). On the robust estimation of spatial autoregressive models. *Econometrics and Statistics*.
- Gatenby, R. A., & Vincent, T. L. (2003). Application of quantitative models from population biology and evolutionary game theory to tumor therapeutic strategies. *Molecular cancer therapeutics*, 2(9), 919-927.
- McGill, B. J., & Brown, J. S. (2007). Evolutionary game theory and adaptive dynamics of continuous traits. *Annu. Rev. Ecol. Evol. Syst.*, 38(1), 403-435.

- Hummert, S., Bohl, K., Basanta, D., Deutsch, A., Werner, S., Theißen, G., ...
& Schuster, S. (2014). Evolutionary game theory: cells as players. *Molecular BioSystems*, 10(12), 3044-3065.
- Traulsen, A., & Glynatsi, N. E. (2023). The future of theoretical evolutionary game theory. *Philosophical Transactions of the Royal Society B*, 378(1876), 20210508.
- Xing, Z., Tan, H. Shi, L. & Zhong, W. (2024+). CALMS: Constrained Adaptive Lasso with Multi-directional Signals for latent network reconstruction. *Neurocomputing*. to appear.

A Proof of Theorem 1

We first define the data transformation to combine network dynamic sequences together into a matrix form for the convenience of notations. Let's denote the vector of responses from n nodes and r -round dynamics as $\mathbf{Y} = [\mathbf{Y}'_1, \dots, \mathbf{Y}'_r]' \in \mathbb{R}^{Nr}$, where $\mathbf{Y}_r \in \mathbb{R}^N$ is the nodal responses in one round of dynamic. $\Phi = [\Psi'_1, \dots, \Psi'_r]' \in \mathbb{R}^{Nr \times N^2}$, and $\epsilon = [\epsilon'_1, \dots, \epsilon'_r]' \in \mathbb{R}^{Nr}$. To be consistent with the classic work in the field of network reconstruction via compressive sensing, we denote the latent network structures as $X \in \mathbb{N} \times \mathbb{N}$, which is the vectorization of the adjacency matrix \mathbf{A} . To keep the notations clear, we denote the dimensions of Φ as (n, p) in the proofs.

Assumption 1. *The unknown true parameter \mathbf{A}^* representing the latent network structures belongs to a compact subset $\mathcal{B} \subseteq \mathbb{R}^{n \times n}$*

Assumption 2. *Every row of the loading matrix Φ_i belongs to a compact set $\mathcal{B} \in \mathbb{R}^p$, $\|\Phi_i\|_2^2 = O_p(p)$*

Assumption 3. *$\frac{1}{n}\Phi'\Phi$ converges to a positive constant matrix Σ*

Assumption 4. *The adaptive weights $\hat{w} = \frac{1}{|\min\{|\tilde{X}|, |\tilde{X}-1|\}|^\gamma}$, where \tilde{X} is a \sqrt{n} -consistent estimator of X^* .*

Assumption 5. *The columns of potential outcome matrix are asymptotically independent, that is, for some given index set Δ , any indexes $i \in \Delta$ and $j \in \Delta^c$, we have $\psi_i^\Delta \perp \psi_j^{\Delta^c}$ when $r \rightarrow \infty$.*

Assumption 6. $\lambda_n/\sqrt{n} \rightarrow 0$ and $\lambda_n n^{(\gamma-1)/2} \rightarrow \infty$.

Lemma 1. *Suppose that $\lambda_n/\sqrt{n} \rightarrow 0$ and $\lambda_n n^{(\gamma-1)/2} \rightarrow \infty$. Under mild assumptions 1, 2, 3, 4, the ALMS estimator defined in (9) satisfies the following:*

1. *Consistency in variable selection:*

$$\mathbb{P}\left(\hat{\mathbf{X}}_{i \in \mathcal{A}_1} = 1\right) \rightarrow 1 \quad \text{and} \quad \mathbb{P}\left(\hat{\mathbf{X}}_{i \in \mathcal{A}_0} = 0\right) \rightarrow 1,$$

where $\mathcal{A}_1 = \{i : X_i^* = 1\}$ and $\mathcal{A}_0 = \{i : X_i^* = 0\}$.

2. *Asymptotic normality:*

$$\sqrt{rn} \left(\hat{\mathbf{X}}_{\mathcal{A}}^* - \mathbf{X}_{\mathcal{A}}^* \right) \xrightarrow{d} \mathbb{N}(\mathbf{0}, \sigma^2 \times \boldsymbol{\Sigma}_{11}),$$

where $\mathcal{A} = \{i, X_i^* \neq 0 \text{ and } X_i^* \neq 1\}$ and $\frac{1}{n} \boldsymbol{\Phi}' \boldsymbol{\Phi} \rightarrow \boldsymbol{\Sigma} = \begin{pmatrix} \boldsymbol{\Sigma}_{11} & \boldsymbol{\Sigma}_{12} \\ \boldsymbol{\Sigma}_{21} & \boldsymbol{\Sigma}_{22} \end{pmatrix}$ is a positive constant matrix and $\boldsymbol{\Sigma}_{11}$ corresponds to the covariates in \mathcal{A} .

Proof. Let's denote the least square estimates (which is not feasible for large-scale networks) of the networks based on the only sub-networks as

$$\hat{\mathbf{A}}_{ols}(Y^\Delta, \boldsymbol{\Psi}^\Delta) = \arg \min_{\mathbf{A} \in \mathbb{R}^{n \times n}} \|\mathbf{Y}^\Delta - (\mathbf{A}^\Delta \circ \boldsymbol{\Psi}^\Delta) \mathbf{1}\|_2^2 \quad (14)$$

and denote the least square estimates of the networks based on the sub-network and its row-component

$$\check{\mathbf{A}}_{ols}^\Delta = \arg \min_{\mathbf{A} \in \mathbb{R}^{n \times n}} \|\mathbf{Y}^\Delta - (\mathbf{A}^\Delta \circ \boldsymbol{\Psi}^\Delta) \mathbf{1} - (\mathbf{A}^{\Delta^c} \circ \boldsymbol{\Psi}^{\Delta^c}) \mathbf{1}\|_2^2 \quad (15)$$

Then based on the true model in (4), the true model for the selected sub-network are:

$$Y^\Delta = (\mathbf{A}^\Delta \circ \Psi^\Delta)\mathbf{1} + (\mathbf{A}^{\Delta_c} \circ \Psi^{\Delta_c})\mathbf{1} + \epsilon^\Delta \quad (16)$$

Then we have

$$vec(\hat{\mathbf{A}}_{ols} - \check{\mathbf{A}}) = [t(\Psi^\Delta)'t(\Psi^\Delta)]^{-1} [t(\Psi^\Delta)'t(\Psi^{\Delta_c})] vec(\mathbf{A}^{\Delta_c}) \quad (17)$$

where $vec(\cdot)$ represents the vectorization of the matrix, $t(\cdot)$ is the data transformation originally defined in Han et al. (2015) and commonly used in literature (Wang et al., 2011; Shi et al., 2021). After the data transformation, we have $t(\Psi^\Delta) \in \mathbb{R}^{n^r \times n^2}$, $t(\Psi^{\Delta_c}) \in \mathbb{R}^{n^r \times (N^2 - n^2)}$, and $vec(\mathbf{A}^{\Delta_c}) \in \mathbb{R}^{(N^2 - n^2) \times 1}$.

From the independence in Ψ based on Assumption 5, we have

$$\lim_{r \rightarrow \infty} t(\Psi^\Delta)'t(\Psi^{\Delta_c}) = 0.$$

As the $t(\Psi^\Delta)'t(\Psi^\Delta)$ will converge to a positive definite matrix, the latent adjacency matrix for binary networks is bounded, we then we have the bias converge to 0 as r goes to infinity. Thus,

$$\hat{\mathbf{A}}_{ols}(Y^\Delta, \Psi^\Delta) \xrightarrow{p} \mathbf{A}^{\Delta*} \quad (18)$$

Now we will show the distributed estimation will enjoy the consistency of the network reconstruction estimator. Let's consider one network estimator based on $\tilde{\mathbf{A}}$ full networks defined in (5) which enjoys the consistency property, then for any given index set Δ , the estimated of the structure in sub-network \mathbf{S}^Δ will be

consistent with the least square estimate

$$\tilde{\mathbf{A}}(Y^\Delta, \Psi^\Delta) \xrightarrow{p} \hat{\mathbf{A}}_{ols}(Y^\Delta, \Psi^\Delta) \quad (19)$$

By the Law of Large Number, we have the consistency properties for $\tilde{\mathbf{A}}$ defined in (6). \square

B Proof of Theorem 2

Proof. Based on the asymptotic normality of the network reconstruction estimator $\tilde{\mathbf{A}}$, let's denote the normality as

$$\sqrt{nr} \left(\tilde{A}_{ij}^b - A_{ij} \right) \xrightarrow{d} N(0, C_{ij}), \quad (20)$$

where $A_{ij} \in \{0, 1\}$ is the true network edge, \tilde{A}_{ij}^b is the classic estimator of A_{ij} based on b -th sub-network and corresponding network dynamics which have the asymptotic variance C_{ij} . Let $c = iN + j$, then $C_{ij} = \Sigma_{c,c}$. Here n is the size of the sub-network and r is a number of dynamic rounds. Based on Assumption 3, the asymptotic variance C_{ij} should be one element in matrix Σ^b .

As there could be some shared nodes in different sub-networks, the two estimators \tilde{A}_{ij}^b and $\tilde{A}_{ij}^{b'}$ can be correlated, where $b, b' \in \{1, \dots, m\}$, and the correlation $\rho_{bb'}$ depends on both the size of network N , the size of sub-network n and also the specific estimation methods used. Therefore, it is nearly impossible to derive a realistic expression for this correlation coefficient. We borrow the idea from the

Breiman (2001) and define the mean of the correlation as

$$\bar{\rho} = \frac{E_{\mathbf{A}^{(b)}, \mathbf{A}^{(b')}}(\tilde{A}_{ij}^b \tilde{A}_{ij}^{b'})}{\sqrt{\text{var}(\tilde{A}_{ij}^b) \text{var}(\tilde{A}_{ij}^{b'})}} \quad (21)$$

where $\mathbf{A}^{(b)}$ and $\mathbf{A}^{(b')}$ are two randomly sampled sub-networks from the population network \mathbf{A} . We have $\bar{\rho} < 1$ when there are at least two different sub-networks.

Then the empirical version

$$\hat{\rho} = \frac{2}{m(m-1)} \sum_{b < b'} \rho_{bb'}$$

will be close enough to $\bar{\rho}$ when number of repeats m is large enough.

Let $m = |\mathcal{G}(i, j)|$, then the distributed estimator of edge A_{ij} is defined as

$$\hat{A}_{ij} = \frac{1}{m} \sum_{b=1}^m \tilde{A}_{ij}^b. \quad (22)$$

define

$$Z_b = \sqrt{rn} \left(\tilde{A}_{ij}^b - A_{ij} \right). \quad (23)$$

and then we have

$$\sqrt{rn} \left(\hat{A}_{ij} - A_{ij} \right) = \sqrt{r} \left(\frac{1}{m} \sum_{b=1}^m \tilde{A}_{ij}^b - A_{ij} \right) = \frac{1}{m} \sum_{b=1}^m Z_b. \quad (24)$$

For any $b \neq b'$, let

$$\text{Cov}(Z_b, Z_{b'}) = C_{ij} \rho_{bb'}, \quad (25)$$

Then

$$\begin{aligned}
\text{Var} \left(\sqrt{r} \left(\hat{A}_{ij} - A_{ij} \right) \right) &= \text{Var} \left(\frac{1}{m} \sum_{b=1}^m Z_b \right) \\
&= \frac{1}{m^2} \sum_{b=1}^m \sum_{b'=1}^m \text{Cov}(Z_b, Z_{b'}) \\
&= \frac{1}{m^2} \left(\sum_{b=1}^m \text{Var}(Z_b) + \sum_{b \neq b'} \text{Cov}(Z_b, Z_{b'}) \right) \quad (26) \\
&= \frac{1}{m^2} \left(m C_{ij} + C_{ij} \sum_{b \neq b'} \rho_{bb'} \right) \\
&= \frac{C_{ij}}{m^2} \left(m + \sum_{b \neq b'} \rho_{bb'} \right).
\end{aligned}$$

Notice that we have $\frac{m(m-1)}{2}$ terms in the summation, and rewrite the summation as

$$\sum_{b \neq b'} \rho_{bb'} = m(m-1) \cdot \frac{\bar{\rho}}{2} = \frac{m(m-1)\hat{\rho}}{2}. \quad (27)$$

Substitute (27) into (26)

$$\begin{aligned}
\text{Var} \left(\sqrt{r} \left(\hat{A}_{ij} - A_{ij} \right) \right) &= \frac{C_{ij}}{m^2} \left(m + \frac{m(m-1)\hat{\rho}}{2} \right) \\
&= C_{ij} \left(\frac{1 - \frac{\hat{\rho}}{2}}{m} + \frac{\hat{\rho}}{2} \right) \quad (28) \\
&\rightarrow \frac{1}{2} C_{ij} \bar{\rho}
\end{aligned}$$

As $\sqrt{rn} \left(\hat{A}_{ij} - A_{ij} \right)$ is the linear combination of $Z_b, b = 1, \dots, m$ which follows normal distribution asymptotically, then

$$\sqrt{rn} \left(\hat{A}_{ij} - A_{ij} \right) \xrightarrow{d} N(0, V), \quad (29)$$

where $V = \frac{1}{2} C_{ij} \bar{\rho}$ given in (28). □